



## Special issue: Research report

# Asymmetry within and around the human planum temporale is sexually dimorphic and influenced by genes involved in steroid hormone receptor activity



Tulio Guadalupe<sup>a,b</sup>, Marcel P. Zwiers<sup>c</sup>, Katharina Wittfeld<sup>d</sup>,  
Alexander Teumer<sup>e</sup>, Alejandro Arias Vasquez<sup>f,g,h</sup>, Martine Hoogman<sup>f</sup>,  
Peter Hagoort<sup>c,i</sup>, Guillen Fernandez<sup>c,h</sup>, Jan Buitelaar<sup>g,h</sup>,  
Hans van Bokhoven<sup>f,h</sup>, Katrin Hegenscheid<sup>j</sup>, Henry Völzke<sup>k</sup>,  
Barbara Franke<sup>f,g</sup>, Simon E. Fisher<sup>a,l</sup>, Hans J. Grabe<sup>d,m</sup> and  
Clyde Francks<sup>a,l,\*</sup>

<sup>a</sup> Language and Genetics Department, Max Planck Institute for Psycholinguistics, Nijmegen, The Netherlands

<sup>b</sup> International Max Planck Research School for Language Sciences, Nijmegen, The Netherlands

<sup>c</sup> Centre for Cognitive Neuroimaging, Donders Institute for Brain, Cognition and Behaviour, Radboud University Nijmegen, Nijmegen, The Netherlands

<sup>d</sup> German Center for Neurodegenerative Diseases (DZNE), Greifswald, Germany

<sup>e</sup> Interfaculty Institute for Genetics and Functional Genomics, University Medicine Greifswald, Greifswald, Germany

<sup>f</sup> Department of Human Genetics, Radboud University Nijmegen Medical Center, Nijmegen, The Netherlands

<sup>g</sup> Department of Psychiatry, Donders Institute for Brain, Cognition and Behaviour, Radboud University Nijmegen Medical Center, Nijmegen, The Netherlands

<sup>h</sup> Department of Cognitive Neuroscience, Donders Institute for Brain, Cognition and Behaviour, Radboud University Nijmegen Medical Center, Nijmegen, The Netherlands

<sup>i</sup> Neurobiology of Language Department, Max Planck Institute for Psycholinguistics, Nijmegen, The Netherlands

<sup>j</sup> Institute of Diagnostic Radiology and Neuroradiology, University Medicine Greifswald, Germany

<sup>k</sup> Institute for Community Medicine, University Medicine Greifswald, Germany

<sup>l</sup> Donders Institute for Brain, Cognition & Behavior, Radboud University Nijmegen, Nijmegen, The Netherlands

<sup>m</sup> Department of Psychiatry and Psychotherapy, HELIOS Hospital Stralsund, University Medicine Greifswald, Greifswald, Germany

## ARTICLE INFO

## Article history:

Received 4 March 2014

Reviewed 19 April 2014

Revised 18 June 2014

Accepted 17 July 2014

Published online 7 August 2014

## ABSTRACT

The genetic determinants of cerebral asymmetries are unknown. Sex differences in asymmetry of the planum temporale (PT), that overlaps Wernicke's classical language area, have been inconsistently reported. Meta-analysis of previous studies has suggested that publication bias established this sex difference in the literature. Using probabilistic definitions of cortical regions we screened over the cerebral cortex for sexual dimorphisms of asymmetry in 2337 healthy subjects, and found the PT to show the strongest sex-linked asymmetry of all regions, which was supported by two further datasets, and also by

\* Corresponding author. Max Planck Institute for Psycholinguistics, Wundtlaan 1, Nijmegen 6525 XD, The Netherlands.

E-mail address: [clyde.francks@mpi.nl](mailto:clyde.francks@mpi.nl) (C. Francks).

<http://dx.doi.org/10.1016/j.cortex.2014.07.015>

0010-9452/© 2014 Elsevier Ltd. All rights reserved.

**Keywords:**

Planum temporale  
 Asymmetry  
 Genome-wide association scan  
 Sexual dimorphism  
 Steroid hormones

analysis with the FreeSurfer package that performs automated parcellation of cerebral cortical regions. We performed a genome-wide association scan (GWAS) meta-analysis of PT asymmetry in a pooled sample of 3095 subjects, followed by a candidate-driven approach which measured a significant enrichment of association in genes of the ‘steroid hormone receptor activity’ and ‘steroid metabolic process’ pathways. Variants in the genes and pathways identified may affect the role of the PT in language cognition.

© 2014 Elsevier Ltd. All rights reserved.

## 1. Introduction

The planum temporale (PT), a triangular shaped area on the superior surface of the posterior temporal lobe, has long been recognized as one of the most anatomically asymmetrical regions of the human cerebral cortex (Geschwind & Levitsky, 1968). In most people the PT on the left side is larger than the right (Galaburda, 1993; Steinmetz, 1996), although varying definitions of the precise structure have resulted in different estimates of its asymmetry (Galaburda, 1993; Shapleske, Rossell, Woodruff, & David, 1999). The left PT overlaps with Wernicke's classically defined language region (Geschwind & Levitsky, 1968), which is part of the broadly left-lateralised speech and language network present in the majority of people. At least some of the PT is regarded as secondary auditory cortex in terms of cyto-architecture (Shapleske et al., 1999). The PT has been characterized as a computational hub for processing spectrotemporal variation in auditory perception (Griffiths & Warren, 2002), as well as having a role in mapping acoustic speech signals to frontal lobe articulatory networks (Hickok & Poeppel, 2007), and in auditory attention (Hirnstein, Westerhausen, & Hugdahl, 2013).

Given these important roles of the PT in speech and language, and its asymmetrical nature in the typically developed brain, there has been much interest in whether individual differences in PT asymmetry are associated with traits that involve changes in language cognition, including dyslexia, reduced verbal ability, and schizophrenia (Eckert et al., 2008; Frank & Pavlakis, 2001; Hasan et al., 2011; Kawasaki et al., 2008; McCarley et al., 2002; Oertel et al., 2010; Shapleske et al., 1999; Sommer, Ramsey, Kahn, Aleman, & Bouma, 2001). These studies have shown that alterations in PT asymmetry may be relevant to some etiological subtypes of these complex traits, although are not necessarily a universal feature of them (Bishop, 2013). It also remains unclear to what extent associations between PT asymmetry and language-related cognitive disorders may arise from shared genetic, versus environmental, influences.

In fact the molecular and developmental basis of human brain asymmetry is almost completely unknown, as are the causes of variation in cerebral asymmetries within the population. Although present to a degree in other primates (Gannon, Holloway, Broadfield, & Braun, 1998; Lyn et al., 2011), a population-level bias towards leftward PT asymmetry is pronounced in the human brain and is already visible in third trimester fetuses (Bossy, Godlewski, & Maurel, 1976). Various other studies have shown foetal and infant asymmetries in the perisylvian region, sylvian fissure, and superior temporal sulcus

(Dubois, Benders, Cachia, et al., 2008; Dubois, Benders, Lazeyras, et al., 2010; Habas et al., 2012; Kasprian et al., 2011; Li et al., 2013). These early developmental asymmetries clearly indicate a role for genetic mechanisms, but very few individual genes have so far been implicated in any aspect of lateralization of the human brain (Francks et al., 2007; Ocklenburg, Beste, & Gunturkun, 2013; Scerri et al., 2011; Sun et al., 2005; Sun & Walsh, 2006). Language lateralization appears to develop largely independently of early embryonic mechanisms that pattern left-right asymmetry of the viscera (heart, lungs etc.; Tanaka, Kanzaki, Yoshibayashi, Kamiya, & Sugishita, 1999). Genetic studies of PT asymmetry therefore offer a potential route to discovering novel, fundamental mechanisms that underlie lateralization of the human brain, which provides a basic organizing principle for much of human cognition (Gunturkun, 2003).

Males have sometimes been reported to show a subtle mean increase in leftward lateralization of the PT relative to females (de Courten-Myers, 1999; Good et al., 2001; Shapleske et al., 1999). Consistent with this, foetal testosterone levels have been linked to gray matter volumes within some putatively, sexually dimorphic regions of the human brain, including the PT (Lombardo et al., 2012). Prenatal testosterone levels have also been implicated in language delay in males (Whitehouse et al., 2012). However, some studies have not found an effect of sex on PT asymmetry (Watkins et al., 2001), and a meta-analysis of thirteen earlier studies did not find significant evidence for sexual dimorphism of PT asymmetry (Sommer, Aleman, Somers, Boks, & Kahn, 2008). Publication bias was suggested to have established a sex difference of PT asymmetry in the literature (Sommer et al., 2008; Watkins et al., 2001). Furthermore, a recent review concluded that overall results from studies on regional grey matter distribution, using voxel-based morphometry (VBM), indicate no consistent differences between males and females in language-related cortical regions (Wallentin, 2009).

In this study we used region-of-interest probability masks derived from the Harvard–Oxford (HO) atlas (distributed with the FSL software package; <http://fsl.fmrib.ox.ac.uk/fsl/>), to perform a large-scale analysis of sex differences for human cerebral asymmetries, mapped over the entire cerebral cortex, in 2337 healthy human subjects. We refer to this method hereafter as HO. We unambiguously confirmed asymmetry within and around the PT as a subtly, sexually dimorphic trait, and this pattern replicated in two additional population samples. We then performed genome-wide association scanning (GWAS) for PT regional asymmetry in three datasets derived from a total of 3095 subjects from the Netherlands and Germany, and used the results to test for an enrichment of

association in genes involved in steroid hormone biology, motivated by the sexual dimorphism of the trait. We also explored the brain-wide effects on grey matter volume of an individual polymorphism that was suggestively associated with PT asymmetry (rs785248,  $p = 1.6 \times 10^{-7}$ , see below), since we do not necessarily expect genetic effects to localize solely to cortical regions as defined in specific brain atlases.

## 2. Methods

### 2.1. Study datasets

The Brain Imaging Genetics (BIG) study was initiated in 2007 and comprises healthy volunteer subjects, including many university students, who participate in studies at the Donders Centre for Cognitive Neuroimaging, Nijmegen, The Netherlands (Franken et al., 2010). At the time of this study the BIG subject-pool consisted of 2337 self-reported healthy individuals (1248 females) who had undergone anatomical (T1-weighted) MRI scans, usually as part of their involvement in diverse smaller-scale studies at the Donders Center, and who had given their consent to participate in BIG. Their mean age was 27.2 years (SD = 12.6; range 18–83). Furthermore, a subset of 242 subjects had undergone a brain MRI scan at least twice. Fifty percent of the rescans took place within 181 days of the first, with the mean elapsed time being 320 days (SD = 360). At the time of the first scan, their mean age was 24.2 (SD = 7.7; range = 18–72).

For the genetic analysis, genome-wide SNP genotype data were available from 1276 of BIG subjects (see below for genotyping details). Their mean age was 22.9 years (SD = 3.8; range = 18–35), and 748 of these subjects were female.

The Study of Health in Pomerania (SHIP) is an on-going, longitudinal, population-based study in north-east Germany, aimed at describing the prevalence of common diseases, and their risk factors. Subjects from the two independent surveys SHIP-2 (the second follow-up of the baseline study SHIP-0) and SHIP-TREND (baseline of the second survey) had undergone a whole-body MRI scan, as well as genotyping for common polymorphisms. For more detailed information about the dataset, see (Volzke et al., 2011). For our analysis we were able to include 935 subjects from SHIP-2 (497 females) with a mean age of 56.7 years (SD = 12.8; range = 31–89) and 888 subjects from SHIP-TREND (495 females) with a mean age of 50.3 years (SD = 13.6; range = 21–81).

### 2.2. Image acquisition

MRI data in BIG were acquired with either a 1.5 Tesla Siemens Sonata or Avanto scanner or a 3 Tesla Siemens Trio or Tim Trio scanner (Siemens Medical Systems, Erlangen, Germany). Given that images were acquired during several smaller-scale

studies, the parameters used were slight variations of a standard T1-weighted three-dimensional magnetization prepared rapid gradient echo sequence (MPRAGE;  $1.0 \times 1.0 \times 1.0$  mm voxel size). See Table 1 for an overview of scanning parameters used in BIG. For the SHIP datasets, all MRI images were obtained on a 1.5 T scanner (MAGNETOM Avanto; Siemens Medical Systems, Erlangen, Germany) using a standard T1-weighted MPRAGE sequence (TE 1900.0, TR 3.4, Flip angle  $15^\circ$ ,  $1.0 \times 1.0 \times 1.0$  mm voxel size) (Hegenscheid et al., 2009).

### 2.3. Image processing

For the analysis of cortical asymmetries MR images were pre-processed using SPM8 (<http://www.fil.ion.ucl.ac.uk/spm/>) in BIG, SHIP-2 and SHIP-TREND. The ‘Segment’ function was used with the default settings to obtain the bias-field corrected, modulated, normalised and warped tissue class images for the grey matter. All of the default options and parameters related to this pipeline can be found on chapter II, ‘Spatial processing’, of SPM8’s manual (<http://www.fil.ion.ucl.ac.uk/spm/doc/manual.pdf>).

Volumetric measures were then extracted by the application of the probabilistic HO Cortical Structural Atlas that defines 48 cortical regions on a normalized brain (as distributed with the FSL software package [http://www.cma.mgh.harvard.edu/fsl\\_atlas.html](http://www.cma.mgh.harvard.edu/fsl_atlas.html)). The cortical parcellations for this atlas were originally described in (Goldstein, Goodman, et al., 1999, Goldstein, Seidman, et al., 2007). We split each of the 48 regions of the HO atlas at the centre of the left-right axis, to produce 48 regions for each cerebral hemisphere. No other manipulation of the atlas or of its probabilistic regions was applied. For each region, we then performed a voxel-wise sum of grey matter volumes, weighted by the probability of each voxel belonging to that specific cortical region. Thirty segmented images were inspected visually using FSLView (<http://fsl.fmrib.ox.ac.uk/fsl/fslview/>) to check for gross errors of segmentation or in the application of the HO atlas, but no errors were identified.

For each cerebral cortical region, volumetric differences between the left and right were expressed as an Asymmetry Index (AI), calculated by the formula  $(L - R)/(L + R)$ , where L and R were the left and right regional grey matter volumes respectively. The values of the AI could range theoretically from  $-1$  to  $+1$ , with negative values denoting a rightward asymmetry, positive values a leftward asymmetry and zero in the case of perfect volume symmetry. Note that regional asymmetries present in the HO atlas would necessarily influence the mean AIs that we measured in our datasets (see below). However, our focus was on individual and group differences in AIs rather than the grand mean, as the left and right perisylvian regions were already known to differ systematically in their anatomy on average. For measuring individual and group differences we needed our left and right atlas

**Table 1 – Overview of the different scanning parameters used in the BIG sample.**

Study sample	TR/T1/TE/sagittal-slices parameters	Scanners	Field strength
BIG	2300/1100/3.03/192; 2730/1000/2.95/176; 2250/850/2.95/176; 2250/850/3.93/176; 2250/850/3.68/176; 2300/1100/3.03/192; 2300/1100/2.92/192; 2300/1100/2.96/192; 2300/1100/2.99/192; 1940/1100/3.93/176 and 1960/1100/4.58/176	Sonata/Avanto, Trio/Trio Tim	1.5 T (N = 634); 3 T (N = 642)

definitions to be as closely anatomically matched as possible to our subject data, and therefore we did not create a left-right averaged template to define the PT, as this fails to adequately capture the systematic anatomical differences between the two sides. In addition we intended to follow up significant genetic associations with individual differences in PT asymmetry, as defined by the asymmetrical HO atlas, by testing the effects of the associated polymorphisms in a brain-wide grey matter VBM analysis without use of atlas-based regional definitions, since we do not necessarily expect genetic effects to be limited to one anatomical region as defined in a particular atlas. Thus the PT AI derived from the HO atlas is a useful initial probe for genetic analysis, but individual genetic effects on this AI then require further analysis to better understand their localization. We return to this issue in more detail in the [Discussion](#).

Exclusion of outlier values (more extreme than 3.5 SD from the mean), correction for covariates (sex, age, total brain volume (TBV), scanner field strength, and scanner), and residual extraction, was done in SPSS (IBM SPSS v.20). We did not include handedness as a covariate because handedness itself is a partly heritable trait ([Medland et al., 2009](#)), and it was therefore important to retain any shared variance of handedness with PT asymmetry, for the purposes of genetic analysis of PT asymmetry.

VBM analysis ([Ashburner & Friston, 2000](#)) was performed within the VBM8 pipeline and toolbox (<http://dbm.neuro.uni-jena.de/vbm/>), implemented in SPM8 (<http://www.fil.ion.ucl.ac.uk/spm/>). All sites followed VBM8's default procedures. First, T1-images were bias-field corrected and segmented into gray, white matter and cerebro-spinal fluid. VBM8's default procedure uses adaptive maximum *a posteriori* estimations and a hidden Markov random field to account for partial volume effects and increase the signal to noise ratio ([Cuadra, Cammoun, Butz, Cuisenaire, & Thiran, 2005](#)). Then, the segmented images were normalized to standard space (as defined by the Montreal Neurological Institute; MNI) by high-dimensional DARTEL warping ([Ashburner, 2007](#)). The resulting images were modulated by the non-linear part of their DARTEL warp field and smoothed with an 8 mm FWHM Gaussian smoothing kernel, providing for an analysis of relative differences in regional GM volume, corrected for individual brain size. A more detailed description of this standard protocol can be found in the VBM8 manual (<http://dbm.neuro.uni-jena.de/vbm8/VBM8-Manual.pdf>).

## 2.4. Parcellation of cortical regions

For a methodological validation we also performed automated parcellation of cerebral cortical regions using the FreeSurfer package ([Fischl et al., 2002](#)) and according to the Destrieux atlas ([Destrieux, Fischl, Dale, & Halgren, 2010](#)), within the 'recon-all' processing pipeline, and using default parameters. This yielded volumetric measures for 74 cortical regions in each hemisphere, for which we also derived AIs and adjusted for covariates as above.

## 2.5. Regional asymmetry mapping by sex

Within the BIG population we used independent sample t-tests to assess sex differences in regional AIs (IBM SPSS

v. 20). Significance levels were conservatively Bonferroni-corrected for all AIs. We did not test for sex differences on bilateral volumes of cerebral cortical regions, as it is well known that males have larger brains on average than females, and this was broadly reflected over the cerebral cortex in our datasets (data not shown).

## 2.6. TBV and asymmetry in the PT region

This analysis was performed in the BIG dataset. We estimated TBV as the voxel-wise sum of the grey matter and white matter probabilities, produced by the segmentation done by SPM8. We then assessed the correlations of sex and TBV with the HO PT AI using Pearson correlation analysis (IBM SPSS v. 20). We also assessed the correlation of TBV with the HO PT AI after removing the effect of sex as a linear covariate, and the correlation of sex with the HO PT AI after removing the linear effect of TBV.

As a confirmatory approach we also assessed the sexual dimorphism of the PT AI using the modulated, non-smoothed, grey matter images produced by the VBM8 pipeline. Because these images were modulated by the non-linear part of the DARTEL field, this results in an assessment of relative volumes corrected for overall brain size.

## 2.7. Genotyping

Genotyping of BIG was performed using the Affymetrix Genome-Wide Human SNP Array 6.0 (Affymetrix Inc., Santa Clara, CA, USA). Genotype calls were made using the Birdseed algorithm ([Rabbee and Speed 2006](#)). Samples were excluded that had call rates lower than 90% and that showed deviant values of genome-wide heterozygosity ([Purcell et al., 2007](#)), as this can indicate the presence of genotyping artifacts. Single nucleotide polymorphisms (SNPs) with a minor allele frequency below 1% or that failed the Hardy–Weinberg equilibrium test at a threshold of  $p \leq 10^{-6}$  were also excluded ([Purcell et al., 2007](#)). The resulting markers were then adjusted to the forward strand, as to avoid any ambiguity problems in subsequent steps. A 2-step imputation protocol was followed, in order to use the genotyped set of markers to infer the genotypes at millions of additional positions in the human genome. We used the software MACH for haplotype phasing and minimac for the final imputation ([Howie, Fuchsberger et al. 2012](#); [Li, Willer et al. 2010](#)), with the 1000 Genomes Phase 1.v3 EUR reference panel ([The 1000 Genomes Consortium, 2012](#)). All monomorphic markers were removed from the reference dataset. Individual genotype calls that had an imputation certainty lower than 90% were removed, as were markers with an overall quality score below .3 R2. As a final quality filter, only markers with no more than 5% missing data were selected. At the end of these procedures, genotypes were available for 1276 subjects from BIG, for 6,131,824 SNPs spanning the genome.

Genotyping of the SHIP-2 and SHIP-TREND samples was done on two different platforms, the Affymetrix Genome-Wide Human SNP Array 6.0 and Illumina Human Omni 2.5, respectively. In SHIP-2 the genotype calling was performed with the Birdseed algorithm and samples were excluded with call rates lower than 86%. For SHIP-TREND, calls were done on



the GenomeStudio Genotyping Module v1.0, and excluded samples had a call rate lower than 94%. For both samples, markers that failed Hardy–Weinberg equilibrium ( $p < 10^{-4}$ ) were removed, as well as markers that had more than 20% and 10% missing data in SHIP-2 and SHIP-TREND, respectively. Imputation of non-observed genotypes was performed on both samples separately, but with the same protocol. The reference panel used, as for the BIG sample, was an all polymorphic 1000 Genomes Phase 1.v3 EUR panel (The 1000 Genomes Consortium, 2012). A two-step approach was used, performed with the software IMPUTE v2.1.2.3 (Howie, Donnelly et al. 2009). This resulted in genotypes for 17,533,349 markers in 932 subjects for SHIP-2 and 17,585,496 markers in 829 subjects for SHIP-TREND.

## 2.8. GWAS

We carried out GWAS using the HO PT AI as a quantitative phenotype, in each of the three datasets, and for males and females separately. In each dataset, only markers that had a minor allele frequency higher than 1%, that were in Hardy–Weinberg equilibrium ( $p > 5 \times 10^{-6}$ ), and had a missing genotype rate lower than 5%, entered the analysis. The association tests were done by linear regression of the HO PT AI on the genotype status separately at each SNP, in an additive genetic model, as implemented in PLINK v1.07 (Purcell et al., 2007).

## 2.9. GWAS meta-analysis

The six sets of GWAS results (i.e., for each of the 3 datasets, and separately for males and females) were meta-analysed per SNP using the ‘sample size’ approach in the software METAL, described in (Willer, Li, & Abecasis, 2010). Put briefly, the meta-analysis pools the probabilities of a genetic effect at each SNP, across each contributing dataset, and weighted by each dataset's sample size, while considering the direction of the allelic effect on the quantitative trait. We chose this method because our six GWAS differed in terms of sex, mean subject age, and other aspects of subject recruitment, so that we wished to avoid assuming an equivalence of estimated genetic effect sizes across datasets and sexes. Finally, we considered only results from SNPs that were present in each of the datasets, resulting in 5,285,490 SNPs genome-wide.

## 2.10. GWAS candidate pathway enrichment analysis

We tested for an enrichment of association with PT asymmetry, of genes involved in steroid hormone biology, using the software INRICH (Lee, O'Dushlaine, Thomas, & Purcell, 2012). Briefly, this approach identifies distinct regions of linkage disequilibrium (LD) in the genome that show association with a trait of interest, below a threshold of nominal significance (we used  $p = .001$ ). The regions of LD are mapped to genes, which are assigned to defined gene sets that represent biological pathways, processes or groups according to prior gene-functional data. Then, regions of LD are shuffled across the genome by permutation (10,000 permutations), to arrive at an empirical measurement of how often the real-data pattern of association within pathways would be observed

by chance alone. This approach is robust to the effect that a gene's or gene set's genomic size has on its probability of containing nominally significant associations. The parameters and options we used were as follows; flanking regions  $\pm 100$  kb; minimum number of genes in pathway 10; maximum 200.

As input we used the results from each of the six GWAS separately, before merging the statistical evidence for each pathway using the ‘sample-size’ approach described earlier (Willer et al., 2010). The  $p$  value for each pathway was then adjusted by Bonferroni correction to compensate for multiple testing over 17 gene sets (see below). A practical constraint that arose from this approach was that we needed to use the LD structure from only one of the datasets (we chose BIG), but there is no reason to expect substantial differences in the genomic distribution of LD between the Dutch and North German populations. We used the Gene Ontology (GO; Ashburner et al., 2000) as our source of assignments of genes to biological pathways. We searched the GO annotation file provided with INRICH for all pathways containing the search terms ‘androgen’, ‘estrogen’, ‘progesterone’, ‘steroid’. 72 pathways were found, of which 16 fulfilled the criteria for association enrichment testing. These pathways were ‘Steroid hormone receptor activity’, ‘Steroid binding’, ‘Steroid biosynthetic process’, ‘Androgen biosynthetic process’, ‘Steroid metabolic process’, ‘Androgen metabolic process’, ‘Estrogen metabolic process’, ‘Steroid hydroxylase activity’, ‘Estrogen receptor binding’, ‘Steroid hormone receptor signalling pathway’, ‘Estrogen receptor signalling pathway’, ‘Androgen receptor signalling pathway’, ‘Response to progesterone stimulus’, ‘Response to estrogen stimulus’, ‘Response to steroid hormone stimulus’ and ‘Androgen receptor binding’.

We also created one additional, custom gene set that comprised the genes listed by (Chakrabarti et al., 2009). This was a manually created gene set containing key genes involved in androgen and estrogen biology.

## 2.11. Meta-VBM analysis of the rs785248 polymorphism

We performed a whole-brain VBM analysis of grey matter volume using the genotypes of the SNP rs785248 within a multiple regression, separately for each of the three datasets and the two sexes. See the Results for an explanation of the choice of this SNP for this analysis. Genotypes were coded as 0, 1 or 2 (i.e., under an additive genetic model) and age and sex were used as covariates (variation in brain volume had already been accounted for in pre-processing – see section 2.3). In BIG, regressors for scanner field strength and scanner were also included as covariates. The resulting statistics were then merged across datasets, separately for each sex and voxel, using the ‘sample-size’ approach described above (Willer et al., 2010). The same approach was then used to meta-analyse both sexes together. To correct for multiple testing across voxels, a false discovery rate (FDR) correction was applied to maintain the family-wise error rate (FWE) at .05 (Genovese, Lazar, & Nichols, 2002). We did not account for multiple testing across males, females, and the sexes combined, since this did not affect the results or interpretation (see below).

### 3. Results

#### 3.1. Sex and cerebral cortical asymmetry

Table 1 shows descriptive statistics of the HO left and right grey matter volumes, and AIs, for regions of the cerebral cortex at which the AI showed a significant mean difference between the sexes (Data for all regions, regardless of an effect of sex on the AI, are given in Supplementary Table A.1). The PT showed the strongest sexually dimorphic asymmetry out of all 48 cortical regions (Table 1). The probabilistic definition of the PT by the HO atlas is illustrated in Fig. 1. The voxels with high probability for mapping to the PT correspond closely with post mortem, neuroanatomical definitions of this structure (Geschwind & Levitsky, 1968; Shapleske et al., 1999; Tzourio-Mazoyer, Simon, et al., 2010). The scan-rescan correlation for the PT AI was high,  $r = .91$ , despite the heterogeneity of scanner and scanning parameters in the BIG dataset, indicating that this heterogeneity had a negligible impact on the measured trait variance. Males had a more pronounced

leftward PT asymmetry than females (Fig. 2). Twelve additional cortical regions also showed significant mean differences of their AIs between the sexes (Table 1). These regions were widely distributed over the cerebral cortex, although they included several temporal regions close to the PT (and for which the regional probability maps sometimes overlapped with that of the PT), such as the anterior divisions of the middle and superior temporal gyri (Table 1). The two population datasets, SHIP-2 (935 subjects) and SHIP-TREND (888 subjects), also supported the PT as having a sexually dimorphic asymmetry, and the magnitudes of the effects of sex in these datasets were consistent with the effect in BIG (Table 2).

SHIP-2 and SHIP-TREND showed decreased PT volumes compared with the BIG dataset (Table 3), but these decreases were consistent with the effect of age on PT volume. Within BIG, we observed linear decreases of PT GM volume with increased age (Supplementary Figure A) that resulted in a volumetric reduction of 13% between the ages of 27 and 53, which are the mean ages of the BIG and SHIP datasets, respectively.

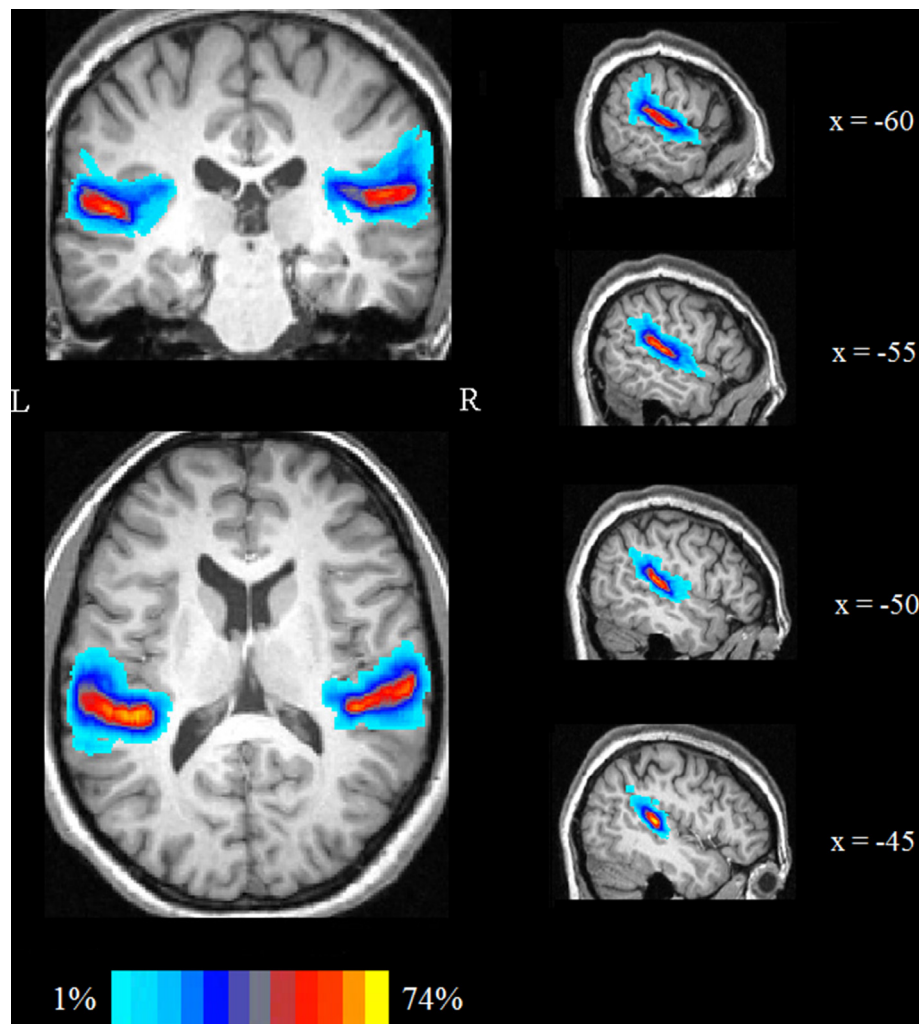
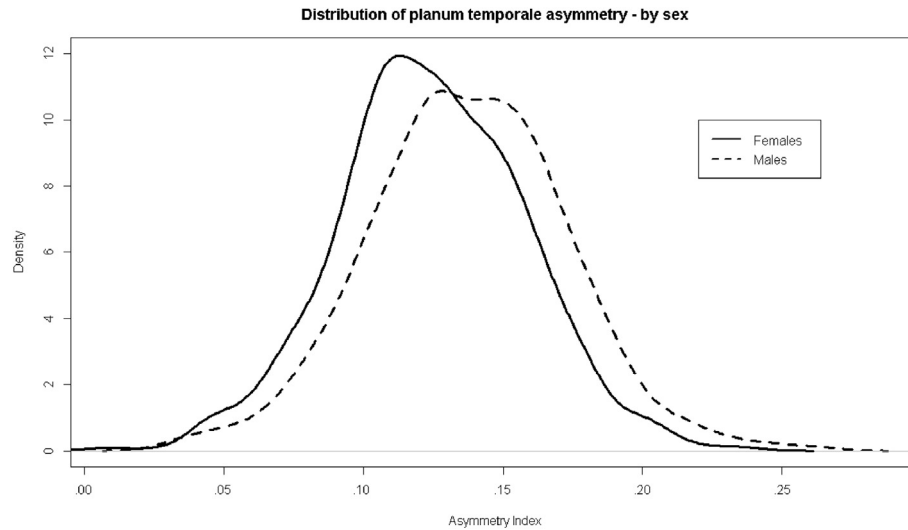


Fig. 1 – The planum temporale as defined with the HO probability mask, from coronal (top left), axial (bottom left), and sagittal (right) views. The sagittal views show the left PT in 4 different slices. The different colours of the mask indicate the voxel probability of belonging to the PT. The image is of a BIG subject for whom the PT AI was .137 (i.e., close to the BIG average AI of .130).



**Fig. 2 – Density plot of the HO planum temporale asymmetry index (PT AI), in the BIG dataset, separately by sex.**

### 3.2. Cortical parcellation with FreeSurfer

With FreeSurfer, the PT showed the third most sexually dimorphic mean AI out of 74 regions defined in the Destrieux atlas, and the neighbouring posterior ramus of the lateral sulcus showed the most significantly sex-linked mean AI (Supplementary Table A.2). However, the FreeSurfer-Destrieux definition of the PT deviates substantially from the classical neuroanatomical definition of this region by extending beyond the horizontal plane to include the vertically-oriented planum parietale (PP; see Supplementary Figure B). This merging of two neighbouring regions in the FreeSurfer-Destrieux atlas was done on the basis of reported cytoarchitectonic similarities between these two regions (Destrieux et al., 2010; Shapleske et al., 1999). However, the asymmetry of the PP was previously found to vary independently of that of the PT (Jancke,

Schlaug, Huang, & Steinmetz, 1994), so that the FreeSurfer-Destrieux merging of these two regions provided a measure that was of limited utility for our further purposes. In addition, the sexual dimorphism of PT asymmetry was weaker for FreeSurfer-Destrieux than for HO, and only one of the SHIP datasets showed a significant effect of sex on PT asymmetry using the FreeSurfer-Destrieux definition (Supplementary Table B). We therefore focussed only on the HO measure of PT asymmetry for subsequent analysis.

### 3.3. TBV and PT asymmetry

Men's brains are well known to be larger on average than women's, and we therefore analysed the link between sex and the HO PT AI in relation to the potentially confounding effect of TBV, using the BIG dataset. Males had a mean TBV of

**Table 2 – Means and standard deviations of grey matter volumes (mm<sup>3</sup>), and Asymmetry Indexes (AI), for Harvard–Oxford atlas regions in the BIG dataset that showed a significant effect of sex on the AI after correction for multiple comparisons. See Table S1 for a description of all regions.**

HO	Males			Females			t-test of AI by sex		
	Left	Right	AI	Left	Right	AI	t-score	p-value	Adj. p-value
Planum Temporale	2035 (278)	1543 (208)	.137 (.036)	1807 (242)	1406 (178)	.124 (.038)	9.05	<.001	<.001
Subcallosal cortex	1759 (194)	2063 (246)	-.079 (.021)	1587 (177)	1889 (222)	-.087 (.021)	8.36	<.001	<.001
Cingulate gyrus, posterior division	3851 (408)	5223 (606)	-.151 (.017)	3448 (367)	4727 (543)	-.156 (.017)	7.57	<.001	<.001
Superior temporal gyrus, anterior division	1002 (125)	1020 (124)	-.009 (.032)	882 (107)	915 (104)	-.018 (.032)	6.95	<.001	<.001
Parietal operculum cortex	2071 (269)	1851 (246)	.056 (.034)	1872 (236)	1704 (214)	.047 (.030)	6.82	<.001	<.001
Lateral occipital cortex, inferior division	6393 (714)	6036 (645)	.028 (.025)	5848 (623)	5463 (568)	.034 (.024)	-5.52	<.001	<.001
Frontal medial cortex	1765 (219)	2123 (286)	-.092 (.021)	1637 (198)	1990 (267)	-.096 (.020)	5.49	<.001	<.001
Occipital pole	5254 (695)	5433 (734)	-.017 (.028)	4779 (585)	4890 (647)	-.011 (.031)	-4.77	<.001	<.001
Middle temporal gyrus, anterior division	1596 (185)	1528 (179)	.021 (.031)	1416 (155)	1370 (149)	.016 (.029)	4.11	<.001	.002
Paracingulate Gyrus	4782 (598)	5301 (761)	-.050 (.022)	4420 (505)	4926 (634)	-.053 (.021)	3.77	<.001	.008
Supracalcarine cortex	791 (107)	1372 (189)	-.268 (.029)	708 (91)	1216 (154)	-.264 (.028)	-3.75	<.001	.009
Cuneal cortex	1628 (220)	2466 (354)	-.204 (.028)	1465 (183)	2196 (290)	-.199 (.030)	-3.69	<.001	.011
Cingulate gyrus, anterior division	4138 (473)	5863 (769)	-.171 (.022)	3781 (407)	5389 (655)	-.175 (.021)	3.64	<.001	.013

**Table 3 – Comparison of Planum Temporale (PT) measures, obtained with HO, across the 3 study datasets. Mean lateral volumes (in mm<sup>3</sup>), and Asymmetry Index (AI) means, are given by sex. The *p* value is shown for testing the effect of sex on the AI.**

		BIG	SHIP-2	SHIP-TREND
Left PT	Males	2035 (278)	1686 (275)	1751 (270)
	Females	1807 (242)	1525 (224)	1574 (234)
Right PT	Males	1543 (208)	1290 (201)	1334 (196)
	Females	1406 (178)	1187 (162)	1226 (174)
PT AI	Males	.137 (.036)	.132 (.034)	.135 (.035)
	Females	.124 (.034)	.124 (.036)	.124 (.33)
<i>p</i> value		<.001	<.001	.002

1315.6 ml, SD 104.6. The female mean TBV was 1171.6 ml, SD 90.0. There was a slight correlation between TBV and PT AI ( $r = .129$ ,  $p < .001$ ). The correlation between PT AI and sex was  $r = -.184$ ,  $p < .001$  (negative  $r$  because males were coded as 1, females as 2). After regressing TBV out of the PT AI, the correlation with sex was slightly decreased, at  $r = -.108$ , though still highly significant,  $p < .001$ . After regressing sex out of the PT AI, then TBV and the PT AI were no longer significantly correlated ( $r = .020$ ,  $p = .34$ ). Consistent with these findings, the correlation between sex and PT AI from the non-linearly modulated GM images (corrected for brain size) was  $r = -.111$ ,  $p < .001$ . These analyses showed that TBV could not explain the majority of the effect of sex on PT asymmetry.

### 3.4. Genetic analysis

The gene set STEROID HORMONE RECEPTOR ACTIVITY (GO:0003707) showed a significant enrichment of association in the GWAS results,  $p = .013$  after adjusting for multiple comparisons across all of the tested pathways. The specific genes in this pathway that contributed to the measured enrichment were: ESR1, ESR2, ESRRA, ESRG, MED12, MED4, NROB1, NR1D2, NR1H3, NR2C1, NR2C2, NR2E1, NR2F1, NR3C2,

NR4A3, NR5A2, PGR, PGRMC2, PPARA, PPARG, RORA, RORB, RXRB, RXRG, THRB and VDR.

In addition, the gene set STEROID METABOLIC PROCESS (GO:0008202) also showed a significant enrichment of association,  $p = .014$  corrected for the multiple pathways tested. In this case, the genes contributing to this association were: ABCA1, AKR1B1, APOB, APOF, CUBN, CYP17A1, CYP19A1, CYP21A2, CYP2A6, CYP2B6, CYP2C19, CYP2C9, CYP2D6, CYP2E1, CYP3A5, CYP3A4, HDLBP, HSD17B3, HSD17B6, HSD19B3, LSS, MBTPS1, NPC1L1, OSBPL10, OSBPL3, OSBPL6, OSBPL7, OSBPL9, PCSK9, SC4MOL, SOAT1, SRD5A1, SREBF1, STAR, STARD5, SULT1A4, SULT1B1, SULT1E1, SULT2B1, UGT1A8, UGT1A1, VLDLR and WWOX.

The GWAS meta-analysis did not identify any individual SNP that surpassed the commonly agreed threshold for calling genome-wide significance of an individual association (threshold  $p = 5 \times 10^{-8}$ ; Fig. 3). There were 4 SNPs that showed suggestive association at a significance level below  $1 \times 10^{-6}$ : rs74462483 ( $p = 1.1 \times 10^{-7}$ ), rs785248 ( $p = 1.6 \times 10^{-7}$ ), rs1971444 ( $p = 7.4 \times 10^{-7}$ ) and rs17074257 ( $p = 8.6 \times 10^{-7}$ ).

The SNP rs74462483 is an intergenic variant on chromosome 13, ~50 kb away from LINC00559 (long intergenic non-protein coding RNA 559) and mir-622 (microRNA 622), with a minor allele frequency (MAF) of .055 (imputation  $r$ -square .92 in BIG). rs785248 is located on chromosome 2 within an intron of C2orf88 (MGC13057) and has a MAF of .29 (imputation  $r$ -squared >.99 in BIG). The messenger RNA of C2orf88 has been shown to be up-regulated in response to knockdown of the progesterone receptor gene in decidualizing endometrial tissue (Cloke et al., 2008), but otherwise little is known of the potential biological functions of C2orf88. rs1971444 is an intergenic variant on chromosome 6, ~50 kb upstream of CDYL, with a MAF = .28 (imputation  $r$ -squared = 1.0). rs17074257 is an intergenic variant located on chromosome 4, and is ~2 kb downstream of DCTD and has a MAF of .27 (imputation  $r$ -square .97 in BIG). The protein encoded by DCTD catalyses the deamination of dCMP to dUMP, the nucleotide

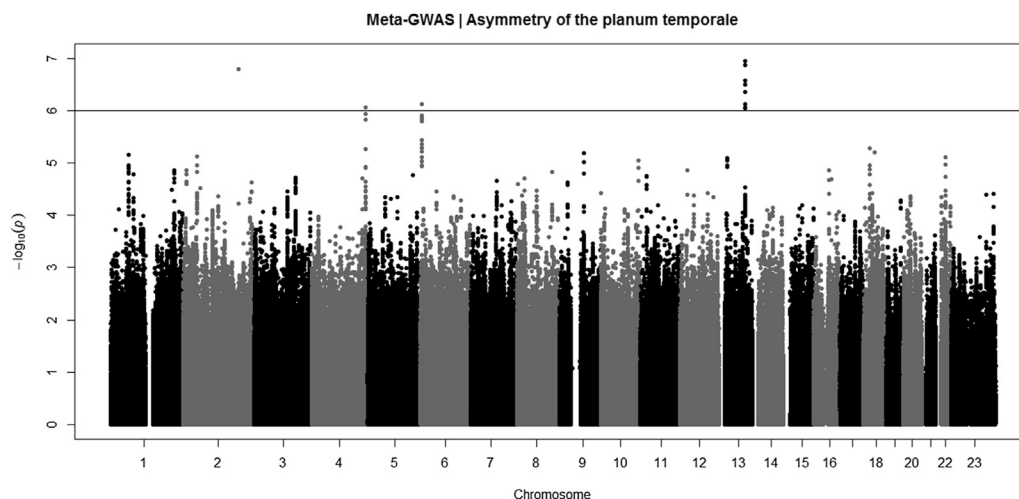


**Fig. 3 – Manhattan plot of GWAS meta-analysis for the HO planum temporale asymmetry index (PT AI). The X-axis represents the chromosomes laid end-to-end, from short to long arms, in ascending numerical order from left to right. The Y-axis shows the pointwise significance of association. The horizontal line represents the threshold we used for suggestive association ( $p = 1 \times 10^{-6}$ ; no result reached genome-wide significance). Shading represents the different chromosomes.**



substrate for thymidylate synthase (Weiner et al., 1995). Table 4 shows the magnitudes of the putative effects for these 4 SNPs in each of the datasets, separately by sex. Each of these 4 SNPs showed a negative direction of effect in each dataset and sex, meaning that the minor allele was associated with a decrease in leftward PT asymmetry. However, the effects were not always statistically significant across all of the datasets and sexes. Of the 4 SNPs, rs785248 showed the most consistency in evidence for association across datasets and sexes, with a significant, negative effect of the minor allele in 4 of the 6 analyses (see Table 4).

### 3.5. Meta-VBM analysis of rs785248

This SNP was selected for brain-wide grey matter VBM association analysis due to the relative consistency of its effect on the PT AI across datasets and sexes, and in light of the link between C2orf88 and the progesterone receptor (Cloeke et al., 2008). This analysis revealed that the effect of this SNP on the PT AI stemmed from a right-sided superior temporal effect that was present in both genders and mapped fairly consistently with the HO definition of PT (Fig. 4). In addition, a cluster of significant voxels was also found in the right inferior frontal lobe (Fig. 5).

## 4. Discussion

GWAS for asymmetry of the PT offers the potential to identify novel molecular and developmental mechanisms that are involved in lateralizing the human brain, for aspects of function that include language. Sexual dimorphism of PT asymmetry has been reported (de Courten-Myers, 1999; Good et al., 2001; Shapleske et al., 1999), but also not found by some studies (Sommer et al., 2008; Wallentin, 2009; Watkins et al., 2001). A sex difference in PT asymmetry would suggest steroid hormone-related genes and pathways as specific candidates for involvement in this asymmetry.

### 4.1. Asymmetry of the PT is sexually dimorphic

In the BIG dataset we screened over the cerebral cortex for regions that showed a mean difference in asymmetry between males and females, using probabilistic definitions for regions of interest. We found that the PT as defined by the HO atlas showed the strongest sexually dimorphic asymmetry of any cortical region, which remained significant when adjusted conservatively for multiple testing over all cortical

regions. Males showed stronger leftward PT regional lateralization than females, which was consistent with some of the larger, previous studies where a sex difference has been reported (de Courten-Myers, 1999; Good et al., 2001; Shapleske et al., 1999; see also a recent study by Ruigrok et al. (2014) showing females to have larger volumes of the right PT than males). The same sexual dimorphism in PT AI that we observed in BIG was also found in the two SHIP datasets, comprised primarily of older adults from north Germany, which totalled 1823 subjects. Of interest to researchers of brain lateralization, handedness was not associated with PT asymmetry; we report elsewhere the results of screening over the entire cerebral cortex in relation to handedness (Guadalupé et al., 2014).

The largest previous study that did not identify a significant sex effect on PT asymmetry (Sommer et al., 2008) was based on meta-analysis of data from 13 separate studies, representing 807 subjects in total. Publication bias was suggested to have established a sex effect on PT asymmetry in the literature (Sommer et al., 2008). Ours is the first study of cerebral cortical asymmetry to have included data from thousands of subjects, while also using relatively uniform methods, and across individually large datasets. The SHIP datasets were population-based samples, thus with minimal selection bias for, or against, potentially confounding factors such as handedness or psychiatric disease. We therefore conclude that a subtle sexual dimorphism of asymmetry within and around the PT is a true feature of the general human population.

Men's brains are well known to be slightly larger on average than women's (Good et al., 2001; Stein et al., 2012), and we also observed this in our datasets. The question arises whether larger brains tend to be more asymmetrical for some regions, independently of sex, which could be a potential confound in measuring sexual dimorphisms of asymmetry (Josse, Herve, Crivello, Mazoyer, & Tzourio-Mazoyer, 2006; Tzourio-Mazoyer, Petit, et al., 2010). While we found evidence that TBV was weakly correlated with PT regional asymmetry, this correlation could not account for the majority of the effect of sex on the asymmetry, and was no longer significant after the effect of sex was removed. We therefore conclude that sex affects asymmetry of the PT via mechanisms that are largely distinct from those determining overall brain size.

The segmentation and normalization steps in the SPM analysis relied on prior information derived equally from both males and females (SPM8 manual; Mazziotta, Toga, Evans, Fox, & Lancaster, 1995), and the HO atlas was also derived from a mixed sample of 21 males and 16 females (Makris et al., 2006; <http://fsl.fmrib.ox.ac.uk/fsl/fslwiki/Atlases>).

**Table 4 – Standardized regression coefficients and p-values, within each dataset and separately by sex, for the 4 SNPs that showed  $p < 10^{-6}$  in the GWAS meta-analysis. Bold values are the nominally significant statistics.**

		rs74462483		rs785248		rs1971444		rs17074257	
		Beta	p	Beta	p	Beta	p	Beta	p
BIG	Females	–.343	.001	–.03	.593	–.105	.064	–.198	>.001
	Males	–.248	.073	–.209	.002	–.089	.196	–.186	.008
SHIP-2	Females	–.396	.006	–.145	.041	–.247	.001	–.087	.226
	Males	–.276	.06	–.21	.004	–.158	.036	–.096	.189
SHIP-T	Females	–.235	.092	–.189	.006	–.08	.25	–.091	.186
	Males	–.205	.138	–.136	.067	–.195	.009	–.122	.095

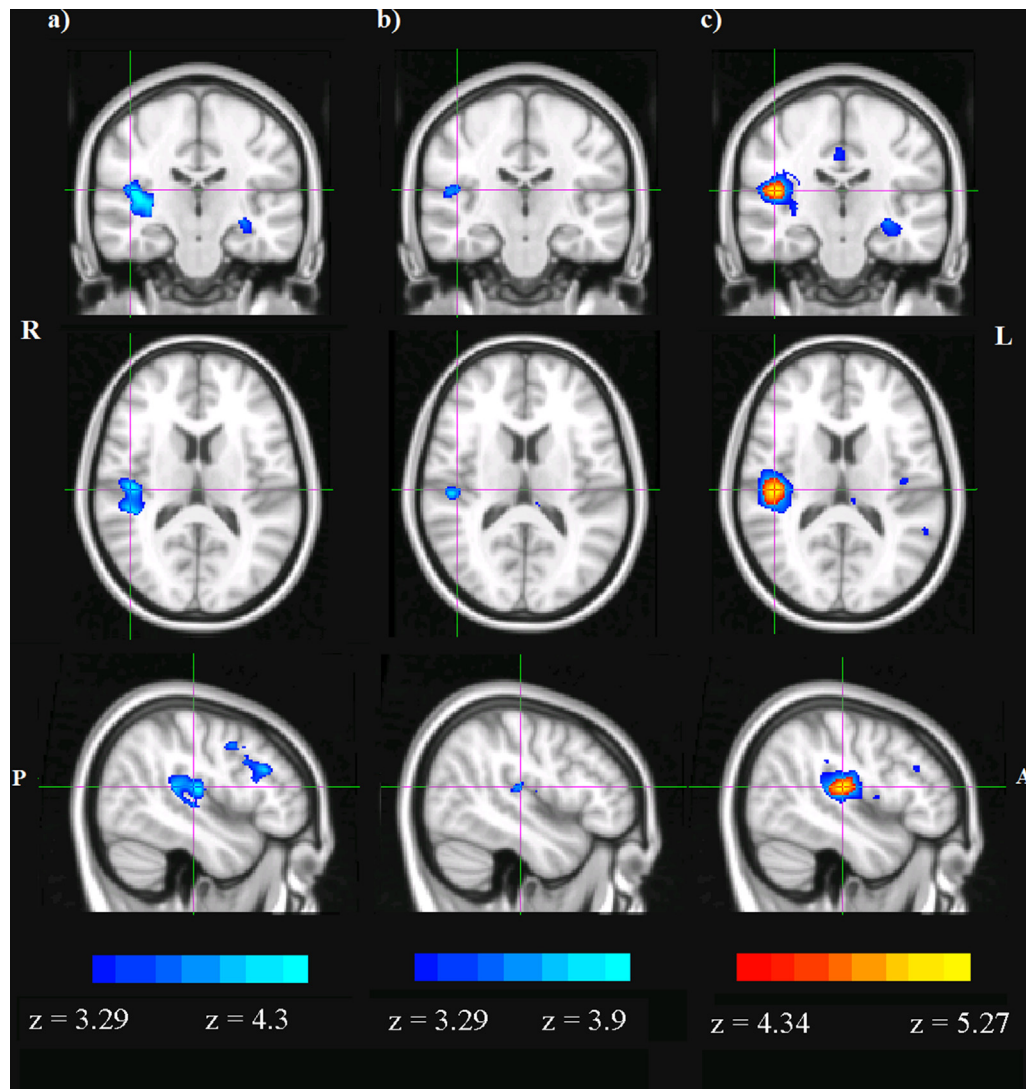


**Fig. 4** – Results of the grey matter VBM analysis of rs785248. Images are shown from 3 different slices, centered on the posterior part of the superior temporal lobe. Depicted in red-orange-yellow (according to their meta-analysed z-score) are the significant voxels after FDR correction brain-wide, while blue shades indicate voxel-wise  $p$  values less than .001 but which did not remain significant after FDR correction. Column (a) depicts the results from males only, column (b) from females and column (c) the results from males and females meta-analysed.

Nonetheless a possible concern is that systematic sex differences in our datasets, for example in gyrification patterns or tissue misclassification, may have contributed to a sex difference being measured in the PT AI. As the effect of sex on the PT AI contributed only 1.2 ~ 1.6% of its variance, it was not feasible to assess these possibilities by visual inspection. Visual checks for gross segmentation errors, or errors in the application of the HO atlas, were carried out for thirty images in the BIG dataset, but in order to characterise a subtle bias explaining 1.2 ~ 1.6% of trait variance then hundreds of images would need to be inspected and measured in detail, and according to criteria that are not clear. Given that the direction of sex effect on the PT AI that we measured agrees with previous neuroanatomical studies when a sex difference was found (as discussed above), we consider it unlikely that an artifact of the image processing pipeline was a main driver of the sexual dimorphism in our data.

The optimised segmentation protocols that we used (Ashburner & Friston, 2005) has its own general limitations regarding such issues as misalignment, the use of templates that are not study-specific, and the degree of non-linear registration (Ashburner, 2009). In order to achieve an adequately powered GWAS meta-analysis, a combined sample of thousands of participants was required (Cantor, Lange, & Sinsheimer, 2010). It was not therefore practical to assess within each dataset how study-specific templates or varying parameters in the optimised protocol might have affected the measurements of cortical asymmetries.

#### 4.2. HO probability map measures individual differences in PT regional asymmetry

The HO atlas was derived from manual segmentations of sets of reference brain images (Destrieux et al., 2010; Goldstein,

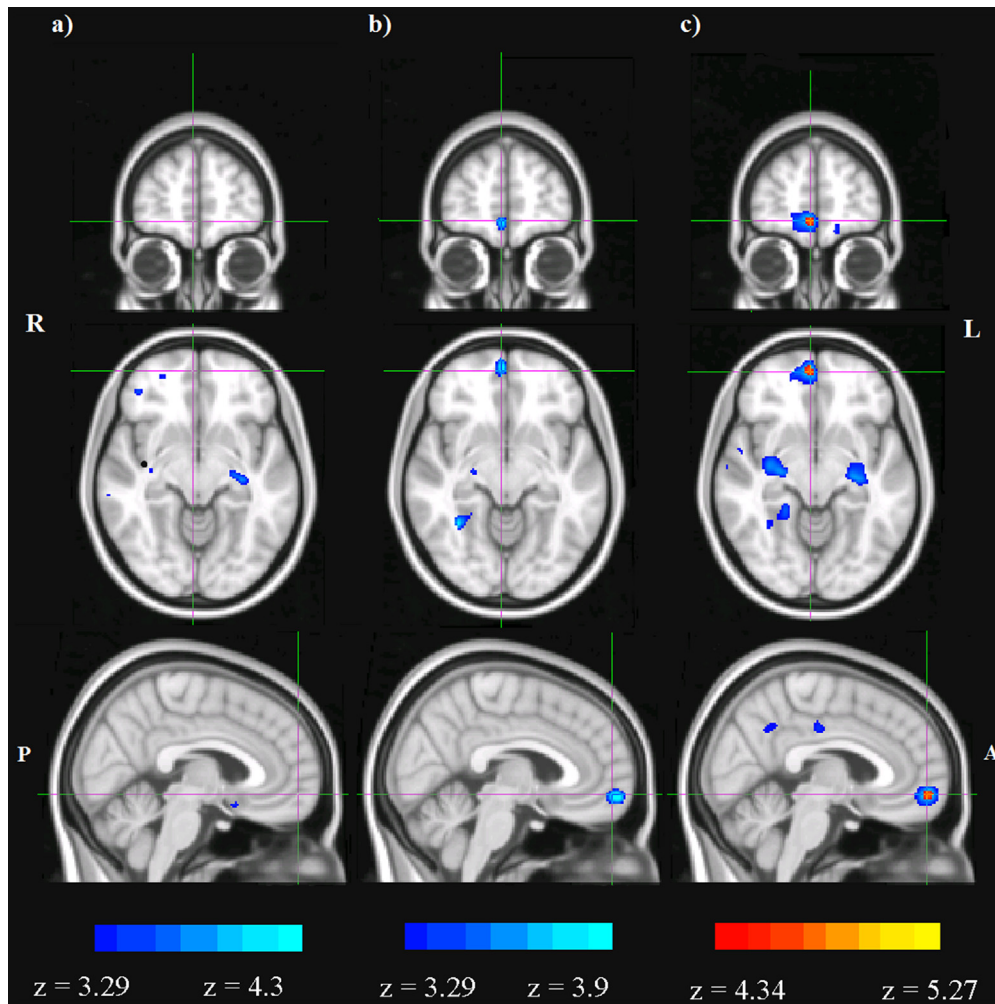


**Fig. 5 – Results of the grey matter VBM analysis of rs785248.** Images are shown from 3 different slices, centered on the inferior part of the prefrontal lobe. Depicted in red-orange-yellow (according to their meta-analysed z-score) are the significant voxels after FDR correction brain-wide, while blue shades indicate voxel-wise p values less than .001 but which did not remain significant after FDR correction. Column (a) depicts the results from males only, column (b) from females and column (c) the results from males and females meta-analysed.

Goodman, et al., 1999; Goldstein, Seidman, et al., 2007). It therefore contained asymmetrical definitions for structures that showed different sizes or locations between the left and right hemispheres in the reference dataset (including the PT; Fig. 1). Accordingly, the measurement of average regional asymmetries in our samples would reflect left-right differences present in the atlas. For detecting cerebral asymmetries with automated methods, some groups have chosen to work from artificially created, left-right symmetrical atlases, e.g., (Kawasaki et al., 2008). However, our study was focused on comparing relative degrees of asymmetry between subjects and groups, i.e., using the individual and group-level differences in the AI, regardless of the mean population level of asymmetry. The use of a ‘real-world’ asymmetrical atlas, rather than an artificially symmetrical atlas, was therefore appropriate for our study, as it had the advantage that regional identification was likely to be more accurate for structures that were asymmetrical both in the atlas and, on average, in our datasets. We did not aim to measure absolute

levels of asymmetry, nor confirm a mean population-level asymmetry of any of the regions under study. In addition, we followed up an interesting SNP association with the HO PT AI by performing brain-wide grey matter VBM association analysis without use of atlas-defined regions of interest (see below). Thus the PT AI derived from an asymmetrical atlas acted as a useful probe for GWAS, but one which necessarily required following up with an atlas-free approach for association signals of interest.

The HO regional probability masks were not constrained in their application by local anatomical features specific to each subject, hence we considered the resulting measures of grey matter volume and asymmetry to reflect regions that were somewhat more inclusive than the target anatomical structures as named in the HO atlas. This expectation was consistent with our observation of no subjects having greater right than left PT volumes, in contrast to classical neuroanatomical studies of the PT which have reported larger right PTs in a minority of subjects (Shapleske et al., 1999). The complete



PT region as defined by HO is larger and more inclusive than the classically defined structure, and therefore indexes a slightly broader regional asymmetry around the posterior sylvian fissure (Fig. 1). However, much of the broader region in the HO atlas was defined at relatively low probability for inclusion in the region, and had correspondingly reduced weight in calculating our volumetric estimates, while the ‘higher probability’ voxels corresponded closely with classical, neuroanatomical definitions of the PT (Fig. 1; Shapleske et al., 1999). The maximum voxel-wise probability for mapping to the PT was 74% in the HO atlas (Fig. 1), illustrating the anatomical variability of the region in the reference brains used for this atlas.

In twice-scanned subjects, for the HO PT AI, we found that the proportion of shared variance between first and second scans ( $r$ -squared) was 81%. This was encouraging for subsequent genetic mapping with this trait, because the repeatability of a measure sets an upper limit on the proportion of trait variance that can be attributed to genetic factors, and has direct implications for the power to detect the effects of polymorphisms in GWAS. Large-scale genetic studies depend on automated methods of image analysis for processing data from very large subject collections, for which manual checking is not an option (Stein et al., 2012). The high repeatability of the HO PT AI, and the consistency of the effect of sex across the datasets that we analysed, indicated that this measure is largely robust to heterogeneity of scanners and scanning parameters, and therefore would be appropriate for even larger GWAS meta-analyses incorporating further datasets.

A practical approach in future genetic mapping may involve the use of multivariate approaches (Ferreira & Purcell, 2009) for analysing asymmetries across multiple, neighbouring regions that are defined within a given atlas, or across multiple atlases as implemented in different automated image analysis methods. However, multivariate approaches are not necessarily straightforward to apply in the context of meta-analysis across multiple datasets.

#### 4.3. Genes involved in steroid hormone biology influence population variance in PT asymmetry

Genes in the GO sets “Steroid Hormone Receptor Activity” and “Steroid metabolic process” were significantly enriched for SNPs showing association with the PT AI, after meta-analysing the results from males and females in the BIG and SHIP datasets. We hypothesise that variants in genes involved in steroid hormone pathways are likely to be downstream modifiers of PT asymmetrical development, rather than directly implicating early embryonic mechanisms that ‘break symmetry’ in the human CNS. Such mechanisms are currently unknown, but are apparently somewhat distinct from those that initiate embryonic left-right patterning of the viscera (heart, lungs etc.; Tanaka et al., 1999). People with left-right *situs inversus* of the viscera are reported to have similar rates of left-lateralised language dominance to people with normally patterned viscera (Tanaka et al., 1999). Visceral asymmetry appears to arise as a consequence of the homochirality (biased handedness) of amino acid molecules in living systems, that together create ‘handed’ cilia leading to a unidirectional, leftward fluid flow within the embryonic node

(Shinohara et al., 2012; Takaoka, Yamamoto, & Hamada, 2007; Yoshida et al., 2012), and ultimately to different gene expression cascades on the two sides of the body. Human CNS asymmetries may also arise from analogous molecular/biophysical asymmetries, but the core mechanism is unknown. Steroid hormone pathways do not present an obvious ‘symmetry breaking’ mechanism. Furthermore, sex clearly has only a modifying effect on the population-level asymmetry within and around the PT, that is nonetheless present and pronounced in both sexes. Therefore, insofar as steroid hormone biology may contribute to the effect of sex on these asymmetries, we conceive of the influence in terms of developmental modulation, rather than a core mechanism that triggers directional CNS asymmetry.

The GWAS meta-analysis also yielded four suggestively associated individual SNPs. The one which showed the most consistent effect across samples and sexes was rs785248, located within an intron of the uncharacterised gene transcript *C2orf88* which has been shown to be affected by manipulation of the progesterone receptor in decidualizing endometrial tissue (Cloeke et al., 2008). This additional, potential link to steroid hormone biology is intriguing in the context of our other genetic findings. The *C2orf88* gene is not contained within the GO sets of “steroid hormone receptor activity” or “steroid metabolic process” genes, and therefore the association at *C2orf88* and the enrichment of association within these GO sets are independent findings that arose from our data.

As there is little reason to expect that a genetic effect will be limited only to one brain region as defined by a particular atlas, we followed up the association within *C2orf88* with brain-wide grey matter VBM-based meta-analysis. This approach allowed a detailed examination of the putative effect of this locus which was free from considerations relating to HO regional definitions and atlas asymmetries. Nonetheless, the results corroborated the HO-based findings and showed rs785248 was associated with the PT AI by affecting GM volume within the right superior temporal region (Fig. 4). While this effect was not significant within each sex separately, when merged by meta-analysis, the putative effect within *C2orf88* was seen for a set of voxels across the right superior temporal gyrus, matching closely the HO definition of PT, as well as within the right medial inferior frontal gyrus (Fig. 5).

The proportion of variance in HO PT AI attributable to rs785248 was roughly .8%, a figure which was largely stable across each of the meta-analysed datasets and both sexes. The concordance of effect size across the datasets supports validity of this potential association, and .8% of trait variance is a realistic size of effect on what is presumably a multifactorial trait that has many contributing genetic and environmental influences (Singleton, Hardy, Traynor, & Houlden, 2010; Stein et al., 2012). Our results clearly rule out the possibility that there exist individual genetic influences on PT regional asymmetry that account for more than a tiny fraction of overall trait variance. This finding is particularly discordant with single-gene theories of human cerebral asymmetry and language (Berlim, Mattevi, Belmonte-de-Abreu, & Crow, 2003). Given the PTs central role in language cognition, variants in the individual genes and steroid-related gene set that we have identified should now be investigated as modifying effects on language and reading performance in clinical and population



samples. We recommend the use of gene-set-based approaches for such follow-up investigations, such as that we have used here (Lee et al., 2012) in which subtle effects of individual variants may be detected in combination. Our data also indicate that larger-scale GWAS meta-analysis of PT regional asymmetry should be pursued, incorporating additional study populations.

An important possibility, for future study, is that sex-linked structural asymmetries in younger females might be dynamically linked to the menstrual cycle, and/or the use of oral contraception which often contains progesterone. Cycle phase-dependent changes in steroid serum levels have been correlated, using functional MRI, with the volume and lateralization of brain activations related to a semantic task, including within the superior temporal cortex (Fernandez et al., 2003). Increased progesterone was linked to more bilateral activation for this task (Fernandez et al., 2003). Menstrual cycle-linked changes in amygdala morphology have also been observed (Ossewaarde et al., 2011). PT leftward asymmetry was slightly reduced in the females of the BIG dataset (many students) as compared to the SHIP datasets (many of whom will have been post-menopausal), which we speculate is consistent with a progesterone-mediated reduction in superior temporal asymmetry.

#### 4.4. Additional sexually dimorphic cerebral asymmetries

Our screen over the entire cerebral cortex for sexually dimorphic asymmetries also identified other sex-linked regions, additional to the PT, some of which have not previously been highlighted in this context (such as the cingulate gyrus). These sex-linked asymmetries were widely distributed over the cortex, and individual differences in these asymmetries, across subjects, were not strikingly correlated with one another (data not shown). The discovery of these additional, sexually dimorphic asymmetries illustrates the power of systematic studies in thousands of subjects to pinpoint subtle group differences. With further validation of their relation to sex, these regional asymmetries may also be considered as candidates for the kinds of genetic analysis that we have performed here in relation to the PT region.

#### Conflicts of interest

No conflicts of interest are declared.

#### Acknowledgements

Many thanks to Nathalie Tzourio-Mazoyer and Fabrice Crivello for advice and critical comments on this manuscript, and to Han Brunner for his involvement in the creation and growth of the BIG (Brain Imaging Genetics) dataset.

The BIG database was established in Nijmegen in 2007. This resource is now part of Cognomics, a joint initiative by researchers of the Donders Centre for Cognitive Neuroimaging, the Human Genetics and Cognitive Neuroscience departments of the Radboud University Medical Centre and the Max Planck

Institute for Psycholinguistics. The Cognomics Initiative is supported by the participating departments and centres and by external grants, i.e. the Biobanking and Biomolecular Resources Research Infrastructure (Netherlands) (BBMRI-NL), the Hersenstichting Nederland and the Netherlands Organisation for Scientific Research (NWO). We wish to thank all persons who kindly participated in this research.

The SHIP datasets are part of the Community Medicine Research net (CMR) of the University of Greifswald, which is funded by the German Federal Ministry of Education and Research and the German Ministry of Cultural Affairs, as well as by the Social Ministry of the Federal State of Mecklenburg–West Pomerania (grants no. 01ZZ9603, 01ZZ0103, and 01ZZ0403), and the network ‘Greifswald Approach to Individualized Medicine (GANI\_MED)’ funded by the Federal Ministry of Education and Research (grant 03IS2061A). Genome-wide data and MRI scans were supported by the Federal Ministry of Education and Research (grant no. 03ZIK012) and a joint grant from Siemens Healthcare, Erlangen, Germany, and the Federal State of Mecklenburg–West Pomerania. The University of Greifswald is a member of the Center of Knowledge Interchange program of the Siemens AG and the Caché Campus Program of the InterSystems GmbH. The SHIP authors are grateful to Mario Stanke for the opportunity to use his Server Cluster for the SNP imputation as well as to Holger Prokisch and Thomas Meitinger (Helmholtz Zentrum München) for the genotyping of the SHIP-TREND cohort.

#### Supplementary data

Supplementary data related to this article can be found at <http://dx.doi.org/10.1016/j.cortex.2014.07.015>.

#### REFERENCES

- Ashburner, J. (2007). A fast diffeomorphic image registration algorithm. *NeuroImage*, 38(1), 95–113.
- Ashburner, J. (2009). Computational anatomy with the SPM software. *Magnetic Resonance Imaging*, 27(8), 1163–1174.
- Ashburner, M., Ball, C. A., Blake, J. A., Botstein, D., Butler, H., Cherry, J. M., et al. (2000). Gene ontology: tool for the unification of biology. The Gene Ontology Consortium. *Nature Genetics*, 25(1), 25–29.
- Ashburner, J., & Friston, K. J. (2000). Voxel-based morphometry—the methods. *NeuroImage*, 11(6 Pt 1), 805–821.
- Ashburner, J., & Friston, K. J. (2005). Unified segmentation. *NeuroImage*, 26(3), 839–851.
- Berlim, M. T., Mattevi, B. S., Belmonte-de-Abreu, P., & Crow, T. J. (2003). The etiology of schizophrenia and the origin of language: overview of a theory. *Comprehensive Psychiatry*, 44(1), 7–14.
- Bishop, D. V. M. (2013). Cerebral asymmetry and language development: cause, correlate, or consequence? *Science*, 340(6138).
- Bossy, J., Godlewski, G., & Maurel, J. C. (1976). Study of right-left asymmetry of the temporal planum in the fetus. *Bulletin de l'Association des anatomistes*, 60(169), 253–258.
- Cantor, R. M., Lange, K., & Sinsheimer, J. S. (2010). Prioritizing GWAS results: a review of statistical methods and recommendations for their application. *American Journal of Human Genetics*, 86(1), 6–22.

- Chakrabarti, B., Dudbridge, F., Kent, L., Wheelwright, S., Hill-Cawthorne, G., Allison, C., et al. (2009). Genes related to sex steroids, neural growth, and social–emotional behavior are associated with autistic traits, empathy, and Asperger syndrome. *Autism Research*, 2(3), 157–177.
- Cloke, B., Huhtinen, K., Fusi, L., Kajihara, T., Yliheikkilä, M., Ho, K. K., et al. (2008). The androgen and progesterone receptors regulate distinct gene networks and cellular functions in decidualizing endometrium. *Endocrinology*, 149(9), 4462–4474.
- de Courten-Myers, G. M. (1999). The human cerebral cortex: gender differences in structure and function. *Journal of Neuropathology and Experimental Neurology*, 58(3), 217–226.
- Cuadra, M. B., Cammoun, L., Butz, T., Cuisenaire, O., & Thiran, J. P. (2005). Comparison and validation of tissue modelization and statistical classification methods in T1-weighted MR brain images. *IEEE Transactions on Medical Imaging*, 24(12), 1548–1565.
- Destrieux, C., Fischl, B., Dale, A., & Halgren, E. (2010). Automatic parcellation of human cortical gyri and sulci using standard anatomical nomenclature. *NeuroImage*, 53(1), 1–15.
- Dubois, J., Benders, M., Cachia, A., Lazeyras, F., Ha-Vinh Leuchter, R., Sizonenko, S. V., et al. (2008). Mapping the early cortical folding process in the preterm newborn brain. *Cerebral Cortex*, 18(6), 1444–1454.
- Dubois, J., Benders, M., Lazeyras, F., Borradori-Tolsa, C., Leuchter, R. H., Mangin, J. F., et al. (2010). Structural asymmetries of perisylvian regions in the preterm newborn. *NeuroImage*, 52(1), 32–42.
- Eckert, M. A., Lombardino, L. J., Walczak, A. R., Bonihla, L., Leonard, C. M., & Binder, J. R. (2008). Manual and automated measures of superior temporal gyrus asymmetry: concordant structural predictors of verbal ability in children. *NeuroImage*, 41(3), 813–822.
- Fernandez, G., Weis, S., Stoffel-Wagner, B., Tendolkar, I., Reuber, M., Beyenburg, S., et al. (2003). Menstrual cycle-dependent neural plasticity in the adult human brain is hormone, task, and region specific. *Journal of Neuroscience*, 23(9), 3790–3795.
- Ferreira, M. A., & Purcell, S. M. (2009). A multivariate test of association. *Bioinformatics*, 25(1), 132–133.
- Fischl, B., Salat, D. H., Busa, E., Albert, M., Dieterich, M., Haselgrove, C., et al. (2002). Whole brain segmentation: automated labeling of neuroanatomical structures in the human brain. *Neuron*, 33(3), 341–355.
- Francks, C., Maegawa, S., Lauren, J., Abrahams, B., Velayos-Baeza, A., Medland, S., et al. (2007). LRRTM1 on chromosome 2p12 is a maternally suppressed gene that is associated paternally with handedness and schizophrenia. *Molecular Psychiatry*, 12, 1129–1139.
- Frank, Y., & Pavlakis, S. G. (2001). Brain imaging in neurobehavioral disorders. *Pediatric Neurology*, 25(4), 278–287.
- Franke, B., Vasquez, A. A., Veltman, J. A., Brunner, H. G., Rijpkema, M., & Fernandez, G. (2010). Genetic variation in CACNA1C, a gene associated with bipolar disorder, influences brainstem rather than gray matter volume in healthy individuals. *Biological Psychiatry*, 68(6), 586–588.
- Galaburda, A. M. (1993). The planum temporale. *Archives of Neurology*, 50(5), 457.
- Gannon, P. J., Holloway, R. L., Broadfield, D. C., & Braun, A. R. (1998). Asymmetry of chimpanzee planum temporale: humanlike pattern of Wernicke's brain language area homolog. *Science*, 279(5348), 220–222.
- Genovese, C. R., Lazar, N. A., & Nichols, T. (2002). Thresholding of statistical maps in functional neuroimaging using the false discovery rate. *NeuroImage*, 15(4), 870–878.
- Geschwind, N., & Levitsky, W. (1968). Human brain: left-right asymmetries in temporal speech region. *Science*, 161(3837), 186–187.
- Goldstein, J. M., Goodman, J. M., Seidman, L. J., Kennedy, D. N., Makris, N., Lee, H., et al. (1999). Cortical abnormalities in schizophrenia identified by structural magnetic resonance imaging. *Archives of General Psychiatry*, 56(6), 537–547.
- Goldstein, J. M., Seidman, L. J., Makris, N., Ahern, T., O'Brien, L. M., Caviness, V. S., Jr., et al. (2007). Hypothalamic abnormalities in schizophrenia: sex effects and genetic vulnerability. *Biological Psychiatry*, 61(8), 935–945.
- Good, C. D., Johnsrude, I., Ashburner, J., Henson, R. N., Friston, K. J., & Frackowiak, R. S. (2001). Cerebral asymmetry and the effects of sex and handedness on brain structure: a voxel-based morphometric analysis of 465 normal adult human brains. *NeuroImage*, 14(3), 685–700.
- Griffiths, T. D., & Warren, J. D. (2002). The planum temporale as a computational hub. *Trends in Neurosciences*, 25(7), 348–353.
- Guadalupe, T., Willems, R. M., Zwiers, M. P., Arias Vasquez, A., Hoogman, M., Hagoort, P., et al. (2014). Differences in cerebral cortical anatomy of left- and right-handers. *Frontiers in Psychology*, 5, 261.
- Gunturkun, O. (2003). In K. Hugdahl, & R. J. Davidson (Eds.), *The asymmetrical brain*. Cambridge, Massachusetts: MIT Press.
- Habas, P. A., Scott, J. A., Roosta, A., Rajagopalan, V., Kim, K., Rousseau, F., et al. (2012). Early folding patterns and asymmetries of the Normal human brain detected from in Utero MRI. *Cerebral Cortex*, 22(1), 13–25.
- Hasan, A., Kremer, L., Gruber, O., Schneider-Axmann, T., Guse, B., Reith, W., et al. (2011). Planum temporale asymmetry to the right hemisphere in first-episode schizophrenia. *Psychiatry Research: Neuroimaging*, 193(1), 56–59.
- Hegenscheid, K., Kuhn, J. P., Volzke, H., Biffar, R., Hosten, N., & Puls, R. (2009). Whole-body magnetic resonance imaging of healthy volunteers: pilot study results from the population-based SHIP study. *Rofo*, 181(8), 748–759.
- Hickok, G., & Poeppel, D. (2007). The cortical organization of speech processing. *Nature Reviews Neuroscience*, 8(5), 393–402.
- Hirnstein, M., Westerhausen, R., & Hugdahl, K. (2013). The right planum temporale is involved in stimulus-driven, auditory attention – evidence from transcranial magnetic stimulation. *PLoS One*, 8(2), e57316.
- Jancke, L., Schlaug, G., Huang, Y., & Steinmetz, H. (1994). Asymmetry of the planum parietale. *NeuroReport*, 5(9), 1161–1163.
- Josse, G., Herve, P. Y., Crivello, F., Mazoyer, B., & Tzourio-Mazoyer, N. (2006). Hemispheric specialization for language: brain volume matters. *Brain Research*, 12(1), 184–193.
- Kasprian, G., Langs, G., Brugger, P. C., Bittner, M., Weber, M., Arantes, M., et al. (2011). The prenatal origin of hemispheric asymmetry: an in Utero neuroimaging study. *Cerebral Cortex*, 21(5), 1076–1083.
- Kawasaki, Y., Suzuki, M., Takahashi, T., Nohara, S., McGuire, P. K., Seto, H., et al. (2008). Anomalous cerebral asymmetry in patients with schizophrenia demonstrated by voxel-based morphometry. *Biological Psychiatry*, 63(8), 793–800.
- Lee, P. H., O'Dushlaine, C., Thomas, B., & Purcell, S. M. (2012). INRICH: Interval-based enrichment analysis for genome wide association studies. *Bioinformatics*, 28(13), 1797–1799.
- Li, G., Nie, J., Wang, L., Shi, F., Lyall, A. E., Lin, W., et al. (2014). Mapping longitudinal hemispheric structural asymmetries of the human cerebral cortex from birth to 2 years of age. *Cerebral Cortex*, 24(5), 1289–1300.
- Lombardo, M. V., Ashwin, E., Auyeung, B., Chakrabarti, B., Taylor, K., Hackett, G., et al. (2012). Fetal testosterone influences sexually dimorphic Gray matter in the human brain. *The Journal of Neuroscience*, 32(2), 674–680.
- Lyn, H., Pierre, P., Bennett, A. J., Fears, S., Woods, R., & Hopkins, W. D. (2011). Planum temporale grey matter asymmetries in chimpanzees (*Pan troglodytes*), vervet (*Chlorocebus aethiops sabaeus*), rhesus (*Macaca mulatta*) and

- bonnet (*Macaca radiata*) monkeys. *Neuropsychologia*, 49(7), 2004–2012.
- Makris, N., Goldstein, J. M., Kennedy, D., Hodge, S. M., Caviness, V. S., Faraone, S. V., et al. (2006). Decreased volume of left and total anterior insular lobule in schizophrenia. *Schizophrenia Research*, 83(2–3), 155–171.
- Mazziotta, J. C., Toga, A. W., Evans, A., Fox, P., & Lancaster, J. (1995). A probabilistic atlas of the human brain: theory and rationale for its development. The International Consortium for Brain Mapping (ICBM). *NeuroImage*, 2(2), 89–101.
- McCarley, R. W., Salisbury, D. F., Hirayasu, Y., Yurgelun-Todd, D. A., Tohen, M., Zarate, C., et al. (2002). Association between smaller left posterior superior temporal gyrus volume on magnetic resonance imaging and smaller left temporal P300 amplitude in first-episode schizophrenia. *Archives of General Psychiatry*, 59(4), 321–331.
- Medland, S. E., Duffy, D. L., Wright, M. J., Geffen, G. M., Hay, D. A., Levy, F., et al. (2009). Genetic influences on handedness: data from 25,732 Australian and Dutch twin families. *Neuropsychologia*, 47(2), 330–337.
- Ocklenburg, S., Beste, C., & Gunturkun, O. (2013). Handedness: a neurogenetic shift of perspective. *Neuroscience & Biobehavioral Reviews*, 37(10 Pt 2), 2788–2793.
- Oertel, V., Knochel, C., Rotarska-Jagiela, A., Schonmeyer, R., Lindner, M., van de Ven, V., et al. (2010). Reduced Laterality as a trait marker of Schizophrenia – evidence from structural and functional neuroimaging. *Journal of Neuroscience*, 30(6), 2289–2299.
- Ossewaarde, L., van Wingen, G. A., Rijpkema, M., Backstrom, T., Hermans, E. J., & Fernandez, G. (2011). Menstrual cycle-related changes in amygdala morphology are associated with changes in stress sensitivity. *Human Brain Mapping*, 34(5), 1187–1193.
- Purcell, S., Neale, B., Todd-Brown, K., Thomas, L., Ferreira, M. A., Bender, D., et al. (2007). PLINK: a tool set for whole-genome association and population-based linkage analyses. *American Journal of Human Genetics*, 81(3), 559–575.
- Ruigrok, A. N., Salimi-Khorshidi, G., Lai, M. C., Baron-Cohen, S., Lombardo, M. V., Tait, R. J., et al. (2014). A meta-analysis of sex differences in human brain structure. *Neuroscience & Biobehavioral Reviews*, 39, 34–50.
- Scerri, T. S., Brandler, W. M., Paracchini, S., Morris, A. P., Ring, S. M., Richardson, A. J., et al. (2011). PCSK6 is associated with handedness in individuals with dyslexia. *Human Molecular Genetics*, 20(3), 608–614.
- Shapleske, J., Rossell, S. L., Woodruff, P. W., & David, A. S. (1999). The planum temporale: a systematic, quantitative review of its structural, functional and clinical significance. *Brain Research. Brain Research Reviews*, 29(1), 26–49.
- Shinohara, K., Kawasumi, A., Takamatsu, A., Yoshida, S., Botilde, Y., Motoyama, N., et al. (2012). Two rotating cilia in the node cavity are sufficient to break left-right symmetry in the mouse embryo. *Nature Communications*, 3, 622.
- Singleton, A. B., Hardy, J., Traynor, B. J., & Houlden, H. (2010). Towards a complete resolution of the genetic architecture of disease. *Trends in Genetics*, 26(10), 438–442.
- Sommer, I. E., Aleman, A., Somers, M., Boks, M. P., & Kahn, R. S. (2008). Sex differences in handedness, asymmetry of the Planum Temporale and functional language lateralization. *Brain Research*, 1206, 76–88.
- Sommer, I., Ramsey, N., Kahn, R., Aleman, A., & Bouma, A. (2001). Handedness, language lateralisation and anatomical asymmetry in schizophrenia: meta-analysis. *British Journal of Psychiatry*, 178, 344–351.
- Stein, J. L., Medland, S. E., Vasquez, A. A., Hibar, D. P., Senstad, R. E., Winkler, A. M., et al. (2012). Identification of common variants associated with human hippocampal and intracranial volumes. *Nature Genetics*, 44(5), 552–561.
- Steinmetz, H. (1996). Structure, functional and cerebral asymmetry: in vivo morphometry of the planum temporale. *Neuroscience and Biobehavioral Reviews*, 20(4), 587–591.
- Sun, T., Patoine, C., Abu-Khalil, A., Visvader, J., Sum, E., Cherry, T. J., et al. (2005). Early asymmetry of gene transcription in embryonic human left and right cerebral cortex. *Science*, 308(5729), 1794–1798.
- Sun, T., & Walsh, C. A. (2006). Molecular approaches to brain asymmetry and handedness. *Nature Reviews Neuroscience*, 7(8), 655–662.
- Takaoka, K., Yamamoto, M., & Hamada, H. (2007). Origin of body axes in the mouse embryo. *Current Opinion in Genetics & Development*, 17(4), 344–350.
- Tanaka, S., Kanzaki, R., Yoshibayashi, M., Kamiya, T., & Sugishita, M. (1999). Dichotic listening in patients with situs inversus: brain asymmetry and situs asymmetry. *Neuropsychologia*, 37(7), 869–874.
- The 1000 Genomes Project Consortium. (2012). An integrated map of genetic variation from 1,092 human genomes. *Nature*, 491(7422), 56–65.
- Tzourio-Mazoyer, N., Petit, L., Razafimandimby, A., Crivello, F., Zago, L., Jobard, G., et al. (2010a). Left hemisphere lateralization for language in right-handers is controlled in part by familial sinistrality, manual preference strength, and head size. *Journal of Neuroscience*, 30(40), 13314–13318.
- Tzourio-Mazoyer, N., Simon, G., Crivello, F., Jobard, G., Zago, L., Percey, G., et al. (2010b). Effect of familial sinistrality on planum temporale surface and brain tissue asymmetries. *Cerebral Cortex*, 20(6), 1476–1485.
- Volzke, H., Alte, D., Schmidt, C. O., Radke, D., Lörbeer, R., Friedrich, N., et al. (2011). Cohort profile: the study of health in Pomerania. *International Journal of Epidemiology*, 40(2), 294–307.
- Wallentin, M. (2009). Putative sex differences in verbal abilities and language cortex: a critical review. *Brain and Language*, 108(3), 175–183.
- Watkins, K. E., Paus, T., Lerch, J. P., Zijdenbos, A., Collins, D. L., Neelin, P., et al. (2001). Structural asymmetries in the human brain: a voxel-based statistical analysis of 142 MRI scans. *Cerebral Cortex*, 11(9), 868–877.
- Weiner, K. X., Ciesla, J., Jaffe, A. B., Ketring, R., Maley, F., & Maley, G. F. (1995). Chromosomal location and structural organization of the human deoxycytidylate deaminase gene. *Journal of Biological Chemistry*, 270(32), 18727–18729.
- Whitehouse, A. J. O., Mattes, E., Maybery, M. T., Sawyer, M. G., Jacoby, P., Keelan, J. A., et al. (2012). Sex-specific associations between umbilical cord blood testosterone levels and language delay in early childhood. *Journal of Child Psychology and Psychiatry*, 53(7), 726–734.
- Willer, C. J., Li, Y., & Abecasis, G. R. (2010). METAL: fast and efficient meta-analysis of genomewide association scans. *Bioinformatics*, 26(17), 2190–2191.
- Yoshida, S., Shiratori, H., Kuo, I. Y., Kawasumi, A., Shinohara, K., Nonaka, S., et al. (2012). Cilia at the node of mouse embryos sense fluid flow for left-right determination via Pkd2. *Science*, 338(6140), 226–312.